Composite Structures 94 (2012) 2246–2253

Contents lists available at SciVerse ScienceDirect

Composite Structures

journal homepage: www.elsevier.com/locate/compstruct

Cyclic responses of reinforced concrete composite columns strengthened in the plastic hinge region by HPFRC mortar

Chang-Geun Cho [a], Yun-Yong Kim [b,*], Luciano Feo [c], David Hui [d]

[a] School of Architecture, Chosun University, Seosuk-Dong 375, Dong-Gu, Gwangju 501-759, South Korea
[b] Dept. of Civil Engineering, Chungnam National University, South Korea
[c] Dept. of Civil Engineering, University of Salerno, Italy
[d] Dept. of Mechanical Engineering, University of New Orleans, USA

ARTICLE INFO

Article history:
Available online 2 February 2012

Keywords:
High Performance Fiber Reinforced Cementitious composites (HPFRCs)
Reinforced concrete composite columns
Multiple-microcracks
Seismic strengthening

ABSTRACT

The brittleness of concrete raises several concerns due to the lack of strength and ductility in the plastic hinge region of reinforced concrete columns. In this study, in order to improve the seismic strength and performance of reinforced concrete columns, a new method of seismic strengthened reinforced concrete composite columns was attempted by applying High Performance Fiber Reinforced Cementitious composites (HPFRCs) instead of concrete locally in the plastic hinge region of the column. HPFRC has high-ductile tensile strains about 2–5% with sustaining the tensile stress after cracking and develops multiple micro-cracking behaviors. A series of column tests under cyclic lateral load combined with a constant axial load was carried out. Three specimens of reinforced concrete composite cantilever columns by applying the HPFRC instead of concrete locally in the column plastic hinge zone and one of a conventional reinforced concrete column were designed and manufactured. From the experiments, it was known that the developed HPFRC applied reinforced concrete columns not only improved cyclic lateral load and deformation capacities but also minimized bending and shear cracks in the flexural critical region of the reinforced concrete columns.

1. Introduction

Due to the increase in number of severe earthquakes in the late 20th century, disaster from the damage/failure of buildings or infrastructures with huge losses of both human life and property is unavoidable. Building or infrastructures built in the past were either designed with a relatively lower level of seismic design load or with no consideration of the seismic design concept, especially in low-rise building/housing structures. Following the increase of damage caused by severe earthquakes all over the world, there is an increased interest in the need for an effective seismic strengthening and rehabilitation of reinforced concrete columns.

The performance of building structures required to resist severe earthquakes mainly depends on the ability of the columns in the lower-stories to sustain relatively large inelastic deformations without a significant loss of load-carrying capacity. However, as shown in Fig. 1, the brittleness and cracking of concrete in the plastic hinge region of reinforced concrete columns raises serious concerns due to the lack of lateral load-carrying and deformation capacities of the column, with the column leading to failure caused by flexural cracks of the concrete, yielding and buckling of the longitudinal bars as well as crushing of the concrete in the plastic hinge zone [1–3].

Steel jacketing in the plastic hinge region of the reinforced concrete column was one of the most well-known strengthening methods, particularly improving the flexural deformation and load-carrying capacities of the columns [4,5]. Fiber wrapping was also perhaps one of the most successful applications of fiber-reinforced polymer (FRP), due to the strength enhancement being accompanied by considerable cost savings over traditional retrofitting alternatives. Fiber reinforced polymer (FRP) could improve the strength and ductility of concrete by confining the concrete [6–9]. A number of studies dealing with improving the strength and ductility of confined concrete wrapped by FRP jackets have been carried out [10–15].

On the other hand, a number of studies have reported that the use of high ductile and high performance cementitious fiber-reinforced composites mortar such as High Performance Fiber Reinforced Cementitious composites (HPFRCs) or Engineered Cementitious Composites (ECCs) can significantly increase the brittleness of concrete in tension. In comparison to normal concrete, the material characteristics of HPFRC, as shown in Fig. 2, retain a high ductile deformation capacity, with a tensile strain of about 2% being caused by multiple fine cracks [16–18]. The development of ECC or HPFRC was primarily motivated by the need to improve a

* Corresponding author. Tel.: +82 42 821 7004; fax: +82 42 821 0318.
E-mail address: yunkim@cnu.ac.kr (Y.-Y. Kim).

0263-8223/$ - see front matter
doi:10.1016/j.compstruct.2012.01.025

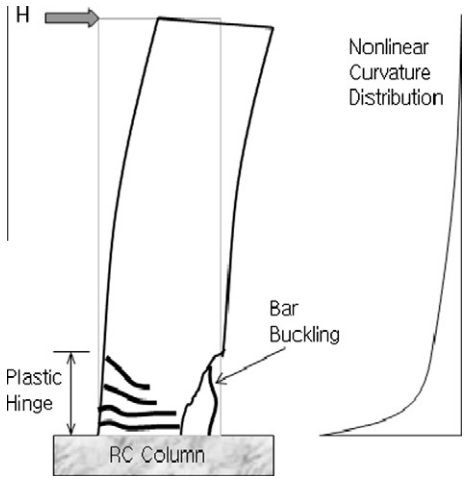

Fig. 1. Plastic hinge in reinforced concrete column.

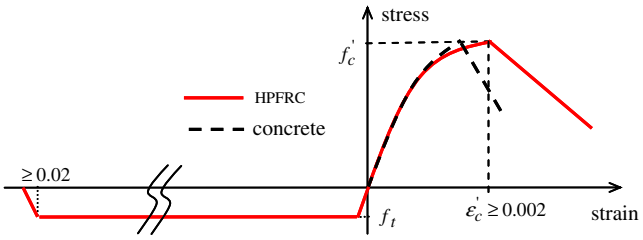

Fig. 2. High-ductile tensile characteristic of HPFRC.

quasi-brittle tensile behavior, which was typical for normal concrete and mortar. HPFRC can be considered a special family of fiber reinforced concrete that exhibits pseudo strain-hardening behavior under uniaxial tension. By increasing the tensile loads, HPFRC generally shows multiple fine cracks of reduced width, without strain localization. Unlike normal concrete, HPFRC can sustain tensile stresses corresponding to high strains [17–19].

In order to improve the seismic performance of reinforced concrete columns, Fischer and Li [20,21] were the first to investigate the effect of the ductile deformation behavior of ECC on the response of both steel reinforced and FRP reinforced columns under reversed cyclic loading conditions. The advantage of applying ECC mortar to concrete flexural members can significantly improve the seismic behavior of concrete building structures, which includes greater deformation and load-carrying capacity, smaller member size, reduced reinforcement and longer span.

The aim of this research is to develop a new approach of seismic strengthened reinforced concrete composite columns by applying HPFRC instead of concrete locally in the region of the column plastic hinge. A series of column tests under cyclic lateral load combined with constant axial load was conducted by manufacturing four specimens: three specimens of reinforced concrete composite cantilever columns by applying HPFRC locally in the column plastic hinge zone with/without tied bars in the zone and one specimen of a conventional reinforced concrete column. By taking into consideration the experimental variables such as applying HPFRC with or without transverse bars, the placed length of HPFRC and the PVA fiber volume fraction in mixing of the HPFRC, the strengthened columns were compared to the conventional reinforced concrete column under a reversed cyclic lateral load. The experimental results reported were used to evaluate the effectiveness of the proposed strengthening concept in the seismic performance enhancement of reinforced concrete columns.

Table 2
Chemical admixtures.

	PCSP	HPMC	Defoamer
Density (g/mm^3)	0.37	0.60	0.26
Type	Brownish powder	White powder	White powder

2. Mixing design and properties of HPFRC

In order to have a high-ductile tensile behavior with multiple microcracks, the HPFRC was freshly mixed in this study by using 1.5% fiber volume fractions with high-tensile Polyvinylalchol (PVA) fibers, ordinary Portland cement (OPC), fine aggregates (maximum grain size 0.25 mm), water, a high-range water-reducing admixture, and admixtures to enhance the fresh properties of the mortar, as shown in Table 1. To increase the matrix fluidity of the cement and fiber dispersibility, a polycarboxylate superplasticizer (PCSP) was used, while hydroxypropyl methylcellulose (HPMC) was also applied to prevent the segregation of materials such as silica, fly ash (FA), blast-furnace slag (BFS) fine powder and fibers. In addition, an antifoaming agent was used to finish the surface as well as control the air content, as shown in Table 2. PVA fibers with a length of 12 mm, a diameter of 39 μm and a surface treated by an oiling agent were used as a reinforcing material to mix the HPFRC mortar in order to improve the brittle nature of the concrete or mortar. The material properties of the PVA fibers are shown in Table 3. The HPFRC as shown in Table 4 had a water/binder ratio (W/B) of 45%, a sand/cement ratio (S/C) of 71%, and a PVA fiber volume fraction of 1.5%.

As shown in Fig. 3, a direct uniaxial tensile test was carried out to evaluate the high-ductile tensile performance of the HPFRC. As shown in the figure, a series of uniaxial tensile tests was carried out using a 10 kN capacity universal testing machine (UTM) by controlling the displacement of 0.2 m/min. The LVDT was attached to two sides of the specimens in order to obtain the tensile strains from the measured displacements. The hardened specimens were removed from the molds 1 day after placing and cured in water for 28 days, with a 30×30 mm cross-section and length of 330 mm.

From the direct uniaxial tensile test, the direct tensile stress and strain relationships of the HPFRC could be measured as shown in Fig. 4. The HPFRC had a high-ductile tensile characteristic, with a measured tensile strain of about 2.5–5.0%. This explained that

Table 1
Properties of mixed materials.

Types	Density (g/mm^3)	Fineness (cm^2/g)	SiO_2	Al_2O_3	Fe_2O_3	CaO	MgO	SO_3	Ig. loss
OPC	3.14	3.200	21.24	5.97	3.34	62.72	2.36	1.97	1.46
Silica sand	2.64	0.2[a]	96.9	1.44	0.34	0.11	0.03	–	–
FA	2.16	3.645	50.5	–	–	–	–	–	3.04
BFS	2.94	4.310	34.7	13.8	0.11	44.6	5.62	0.23	0.64

[a] Diameter (mm).

Table 3
Properties of PVA fiber.

Ingredient	Density (g/mm^3)	Length (mm)	Diameter (μm)	Surface treatment	Tensile strength (MPa)	Young's modulus (GPa)	Elongation (%)	Alkali resistance
Polyvinylalchol (PVA)	1.3	12	39	Oiling agent	1600	40	3–113	High

Table 4
Mixing properties of HPFRC.

W/B wt.%	S/C (wt.%)	FA/B (wt.%)	Slag/B (wt.%)	Unit: kg/m^3									
				W	B[a]	OPC	FA	BFS	Silica sand	PCSP	HPMC	Defoamer	PVA (vol.%)
45	71	20	20	375	833	500	167	167	692	0.37	0.18	0.45	1.5

[a]B: OPC + FA + BFS.

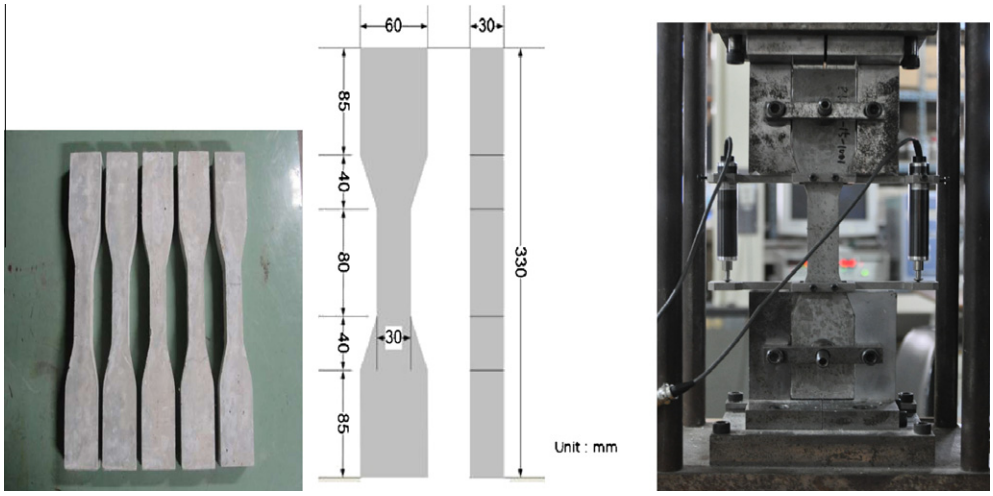

Fig. 3. Setup for direct tensile test of HPFRC specimens.

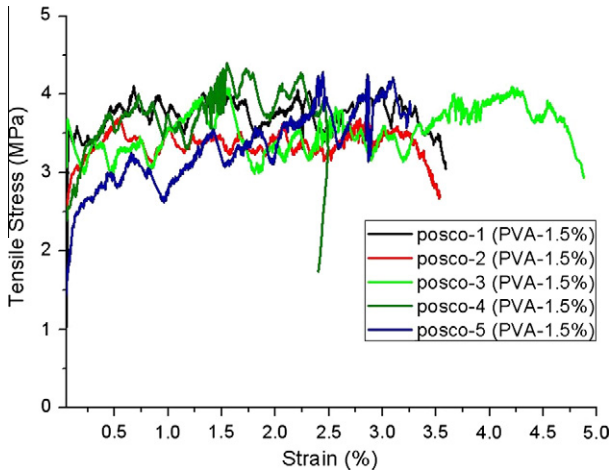

Fig. 4. Measured tensile stress–strain behaviors of HPFRC specimens.

the high-ductile tensile behavior after cracking of the HPFRC could be caused by the appearance of multiple microcracks as shown in Fig. 5. An apparent curing strain behavior was also observed after the premature cracks, which seemingly displayed the properties of high toughness since it had a relatively improved resistance to concrete when the cracks appeared. The premature cracking strength was approximately 1.7–3.7 MPa, while the maximum tensile strength measured in the interval of the curing behavior was 3.7–4.4 MPa. The results highlight that the HPFRC had the mechanical characteristics of a high-ductile tensile strain with multiple microcracks, thus improving the brittleness of the concrete.

3. Experimental program of strengthened columns

3.1. Design and manufacture of column specimens

In order to improve the lateral load-carrying and deformation capacities of the reinforced concrete columns, the current strengthening method is that the column section from the column base to above the length of the plastic hinge region is placed by the HPFRC instead of concrete with and without transverse reinforcements. Four specimens were manufactured, representing the first-storey column between the footing and the inflection point, with the column being fixed to the column base as the cantilever column. Three specimens were strengthened with reinforced concrete composite columns by applying HPFRC locally in the column plastic hinge zone and one specimen as the conventional reinforced concrete column. Table 5 summarizes the four specimens with the design variables and Fig. 6 illustrates the geometry and reinforcement details of the specimens. The main variables in this

Fig. 5. Multiple micro-cracks of HPFRC specimens.

Table 5
Variables of column specimens.

Specimen name	Fiber volume fraction (V_f)	Height of HPFC	Reinforcements (main/shear)
RC-0	–	–	8-D13/D10 @ 100
HPFC-RC-0	PVA (1.5%)	$H = 2.0d$	8-D13/D10 @ 100
HPFC-RC-1	PVA (1.5%)	$H = 2.0d$	8-D13/no stirrup
HPFC-RC-2	PVA (2.0%)	$H = 1.5d$	8-D13/D10 @ 100

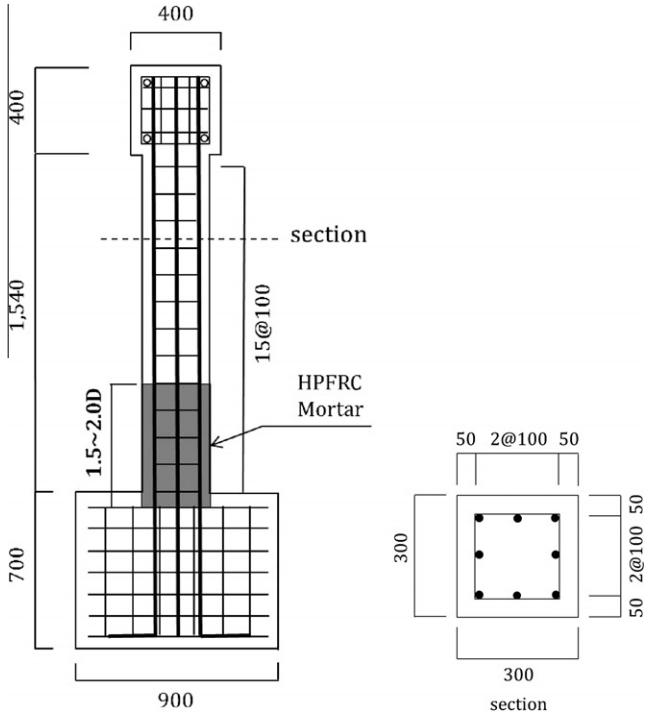

Fig. 6. Geometry and reinforcement details of column specimens.

(a) Form work (b) Assembling reinforcements

(c) attaching gauges (d) Placing reinforcements

(e) Mixing HPFRC (f) Placing HPFRC

(g) Placing topping concrete and curing

Fig. 7. Manufacturing process of column specimens.

experiment were the PVA fiber volume fraction, the length of HPFRC and the amount of shear reinforcements. Each column had a 300 mm × 300 mm cross-section, height of 1540 mm, a 400 mm × 400 mm cross-section of the head part of the column and the column base which was connected to a reinforced concrete footing, measuring 900 mm × 900 mm × 700 mm. The cross-section for all of the specimens had a main longitudinal reinforcements as eight units of D13 bars.

The standard specimen RC-0 is a conventional reinforced concrete column. In order to evaluate the strengthening effect of HPFRC, with a detailed design variable of each specimen as shown in Table 5, the specimens HPFC-0, HPFC-1, and HPFC-2, the HPFRC were manufactured by assembling and placing the HPFRC with a length of 1.5–2.0d from the column base with or without transverse reinforcement, where d is the effective depth on the cross-section of

(a) Side view (b) Frontal view

Fig. 8. Setup for cyclic load test of columns.

the column. In the column base, in order to avoid failure induced by construction joint between the concrete in the footing and the HPFRC, the HPFRC was placed about 50 mm inside the footing. For specimen HPFC-1, the shear reinforcements were not placed at the height of the HPFRC in order to evaluate the control of shear cracks by HPFRC, while for all the other cases, the shear reinforcements were assembled with D10 bars with a space of 100 mm. The topping concrete was placed with finishing after placing the HPFRC. The practical manufacturing process of the specimens is shown in Fig. 7.

3.2. Properties of the concrete and reinforcing steel bars

Two types of reinforcing steel bars produced in Korea were used in the column specimens. The yielding stresses of the reinforcing bars for the main longitudinal bars (D13) and the transverse bars (D10) measured 385 MPa and 383 MPa, respectively. The concrete was mixed with OPC, crushed stones with a maximum aggregate size of 20 mm, sand and admixtures. The combinations of the concrete mixtures were designed to satisfy the required strength, workability, and mechanical characteristics of the selected concrete. Cylindrical specimens were cast to test the compressive strength of the concrete, with each specimen using $\varnothing 100 \times 200$ mm molds by placing the concrete in three layers and then externally vibrated. The specimens were wrapped with plastic immediately after production and moist-cured for 28 days. The uniaxial compressive strength of the concrete was measured as the average of 28.7 MPa.

3.3. Experimental procedure

The installation of the test frame for the column specimens is shown in Fig. 8. To provide cantilever-type loading conditions, the bottom stub of each specimen was fixed to the base in order to achieve fully fixity at the base.

This loading configuration was chosen to promote a flexural deformation mode in all the specimens as well as investigate the effect of the HPFRC material properties on the expected plastic hinge region in particular. Lateral loading was applied through a reaction wall equipped with a 100 kN-capacity actuator according to a predetermined displacement-controlled loading sequence. Fig. 9 illustrates the unidirectional lateral displacement history followed in the testing specimens. The cyclic lateral load was controlled by the top-displacement of the column by μ, the laterally displacement ductility ratio defined as the ratio of the current displacement to the yielding displacement of the column. To apply axial loading, external steel tendons were attached between the pin and the loading frame and tensioned by hydraulic actuators. The axial load of the column was set to 196.2 kN during the loading history. The specimens were equipped with a displacement transducer at the top of the column to measure and control the lateral displacement of the column. The strain gauges were attached to the longitudinal and transverse reinforcing bars, with the space of the transverse reinforcements from the column base to the height being 2.0*d*.

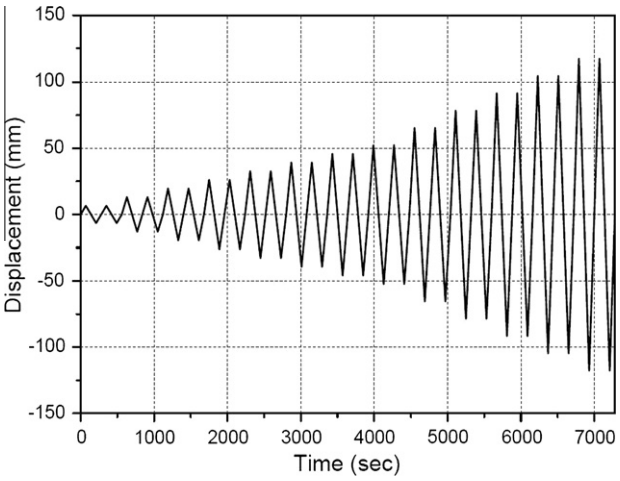

Fig. 9. Cyclic lateral loading history by displacement control.

4. Evaluation of cyclic load test of column

4.1. Hysteretic behaviors, displacement ductility and evaluation of seismic strengthening

In order to evaluate the seismic responses of the reinforced concrete columns in severe earthquake regions, it is necessary to understand the seismic performance characteristics of the column, such as ductility, energy dissipation capacity, strength deterioration, and stiffness degradation. For this reason, the hysteretic behavior of the members should be thoroughly investigated. Fig. 10 shows the lateral load–top displacement hysteretic behavior of each column. For the specimens HPFR-0, HPFR-1, and HPFR-2, since the limited displacement capacity of the actuator is up to ± 150 mm, the displacement-controlled cyclic loading was stopped if the lateral top displacement of the column reached about 120 mm.

In comparison to the conventional reinforced concrete column, RC-0, the developed strengthened columns, HPFR-0, HPFR-1, and HPFR-2, could provide excellent seismic improved responses in improving the load-carrying and deformation capacities of the column during cyclic load reversals.

The primary curve of each specimen as shown in Fig. 11 can be obtained from the lateral load–top displacement hysteretic behavior of each specimen, and Table 6 provides a summary of the

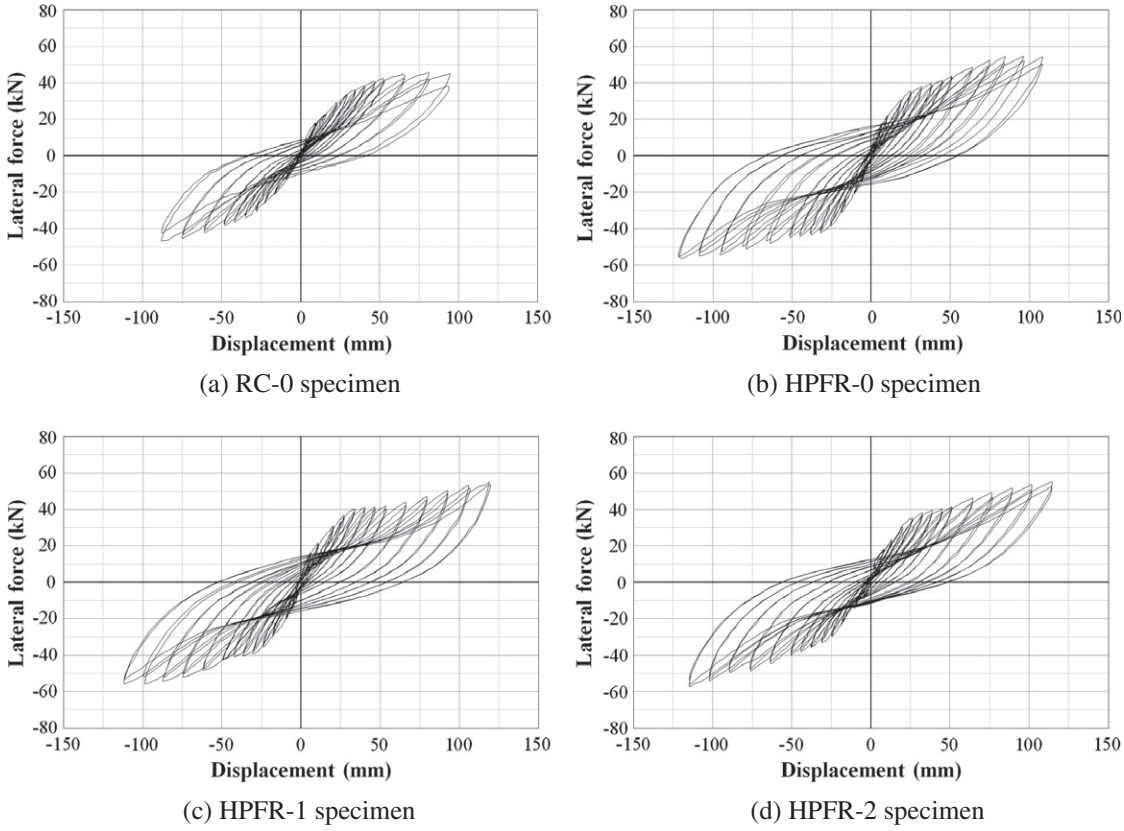

Fig. 10. Cyclic lateral load–top displacement responses of columns.

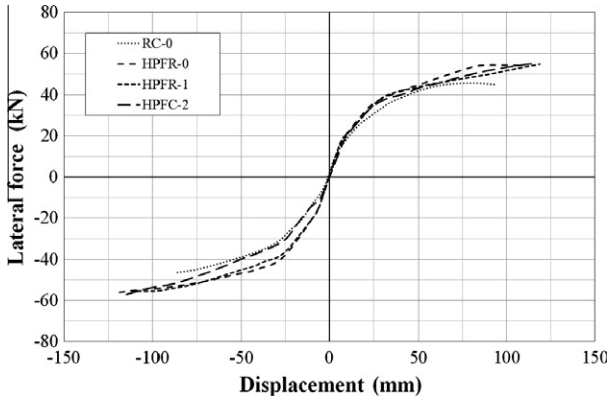

Fig. 11. Primary lateral load–top displacement curves of columns.

measured overall primary responses of each column. In comparison to the conventional reinforced concrete column, RC-0, the ultimate lateral loads of the specimens HPFR-0, HPFR-1, and HPFR-2 were improved by about 34.8%, 22.0%, and 44.8%, respectively. For the three specimens HPFR-0, HPFR-1 and HPFR-2, the maximum lateral top-displacements exceeded 120 mm which was the allowable displacement capacity of the actuator. However, the maximum lateral top-displacement of the specimen RC-0 reached 91.6 mm.

In the case of the hysteretic response of each specimen, in comparison to RC-0, the three specimens HPFR-0, HPFR-1, and HPFR-2 showed improved and stable hysteretic responses in increasing the energy dissipation capacity and reducing the strength deterioration and stiffness degradation of the column during the reversed cyclic load.

4.2. Cracks and failure patterns

The crack and failure patterns of each column from the frontal and side view are shown respectively in Figs. 12 and 13. For the specimen RC-0 initial bending cracks near the column base appeared at the load level of $\pm 0.5\delta_Y$ (two cycles) and the number of bending cracks gradually augmented according to the increase of the cyclic loading. After the load level of $\pm 1.5\delta_Y$ (five cycles), the width of the bending cracks notably increased but the number of cracks did not. In the load level of $\pm 2.0\delta_Y$ (eight cycles), additional bending cracks appeared near the column joint. Upon increasing the cyclic loads, cracks, spalling of the cover concrete and buckling of the longitudinal bars were observed near the zone of the column

Table 6
Summary of characteristics of HPFRC mortar.

Specimen name	Initial crack		Yielding of bar		Max. displacement		Variation of load (%)	Ductility ratio
	disp. (mm)	load (kN)	disp. (mm)	load (kN)	disp. (mm)	load(kN)		
RC-0	4.6	17.2	18.6	28.2	91.6	44.9	–	4.2
HPFR-0	4.7	15.4	19.4	26.3	121.9	60.6	+34.8	6.3
HPFR-1	4.5	13.5	18.2	28.4	118.7	54.8	+22.0	6.5
HPFR-2	4.9	14.2	18.2	23.6	116.8	65.1	+44.8	6.4

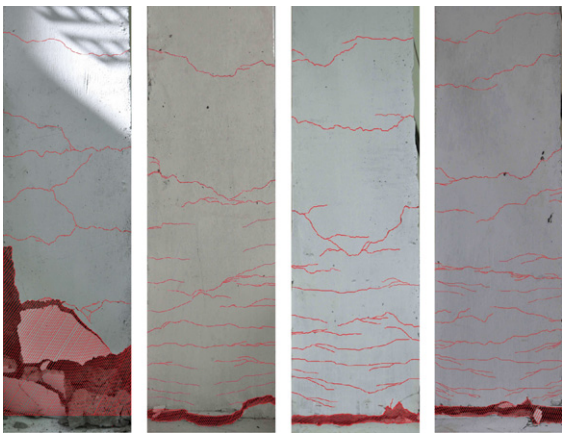

(a) RC-0 (b) HPFR-0 (c) HPFR-1 (d) HPFR-2

Fig. 12. Crack patterns at failure (frontal view).

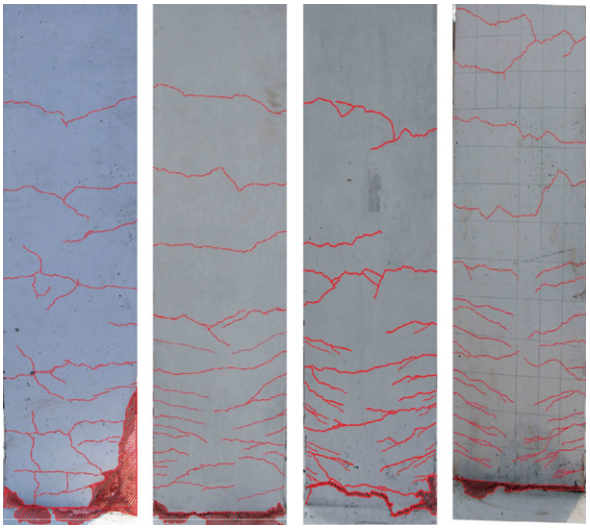

(a) RC-0 (b) HPFR-0 (c) HPFR-1 (d) HPFR-2

Fig. 13. Crack patterns at failure (side view).

plastic hinge from the column base to the length of effective depth (d) in the direction of column axis. The maximum lateral load-capacity was reached near the load level of $\pm 6.0\delta_Y$ (19 cycles), and it was observed after the load level that the shear cracks were extended near the height of 2.0d from the column base, the expansion and spalling of the concrete with buckling of the longitudinal bars appeared near the length of 1.0d from the column base. The specimen finally reached failure by accumulated bending cracks during the loading history combined with shear cracks appearing near the ultimate load level.

For the specimen HPFR-0, the HPFRC with the PVA fiber volume fraction of 1.5% was placed along the length of 2.0d from the column base and D10 transverse bars with a spacing of 100 mm were applied. At the load level of $\pm 0.5\delta_Y$ (two cycles), microcracks by bending on the surface of the HPFRC initially appeared near the column base. After the load level of $\pm 1.5\delta_Y$ (six cycles), the number of multiple microcracks on the surface of the HPFRC gradually increased. A number of bending cracks rapidly appeared upon reaching the level of $\pm 4.0\delta_Y$. However, a more noteworthy increase of the crack width was observed after the load level. The maximum lateral load-capacity of the column was reached near the load level of $\pm 8.0\delta_Y$ (23 cycles). Unlike the specimen RC-0, the shear cracks were not observed during loading history, the spalling and damage of the cover concrete near the zone of plastic hinge were not as serious, and the specimen reached failure by bending cracks near the column base.

For the specimen HPFR-1, the HPFRC with the PVA fiber volume fraction of 1.5% was placed along the length of 2.0d from column base but the transverse bars were not applied along the length of the HPFRC. Initial microcracks by bending on the surface of the HPFRC appeared near the column base at the load level of $\pm 0.5\delta_Y$ (two cycles). At the load level of $\pm 1.5\delta_Y$ (five cycles)–$\pm$ 2.5δ_Y (nine cycles), a number of multiple microcracks on the surface of the HPFRC appeared in the zone of plastic hinge, with the crack width being magnified after reaching the load level of $\pm 4.0\delta_Y$ (16 cycles). The specimen reached the maximum lateral load-capacity at the load level of $\pm 8.0\delta Y$ (24 cycles). In spite of no transverse reinforcements in the length of the HPFRC, the shear cracks were not observed on the surface of the HPFRC and damage of the specimen was not as serious when compared to the specimen RC-0.

For the specimen HPFR-2, the HPFRC with the PVA fiber volume fraction of 2.0% was placed along the length of 1.5d from column base and the D10 transverse bars with a spacing of 100 mm were applied. As with the other specimens, microcracks by bending on the surface of the HPFRC were initiated at the load level of $\pm 0.5\delta_Y$ (two cycles), and the multiple microcracks on the surface of the HPFRC were widely spread at the load levels from $\pm 1.5\delta_Y$ (five cycles) to $\pm 2.0\delta_Y$ (seven cycles). After reaching the load level of $\pm 4.0\delta_Y$ (15 cycles), a number of bending cracks increased and the width of the cracks gradually augmented. The specimen reached the maximum lateral load-capacity at the load level of $\pm 9.0\delta_Y$ (25 cycles). Until the specimen reached failure by bending, shear cracks on the surface of HPFRC could not be observed and spalling of the cover concrete, damage of the concrete, and buckling of the bars were not as serious when compared to the specimen RC-0.

5. Conclusions

A method for the seismic strengthening of reinforced concrete composite columns was introduced by applying HPFRC, a newly mixed high-ductile fiber-reinforced cementitious composite in this study, and a series of cyclic load tests of the columns was carried out in order to evaluate the strengthened composite column method. The following conclusions can be made on the basis of the experimental results.

In this strengthening method, the HPFRC was locally placed instead of concrete on the length of 1.5–2.0d from the column base in the flexural critical region as the zone of column plastic hinge. Three specimens of strengthened columns were sufficient to improve the overall lateral load-carrying and deformation capacities when compared to the conventional reinforced concrete column specimen.

In comparison to the conventional reinforced concrete column specimen, by locally applying the HPFRC instead of concrete near the flexural critical region, the concentrated local damage of the reinforced concrete columns in the zone of the column plastic hinge induced by bending and shear cracks of the concrete, spalling of the cover concrete, buckling of the longitudinal reinforcing bars, and compressive crushing of the concrete could be minimized so that the overall lateral performances of the reinforced concrete columns could be improved. It was known that the HPFRC mixed in this study had high-ductile tensile strains about 2.0–4.5% with the behavior of multiple microcracks under direct uniaxial tensile tests so that the HPFRC was effective to control bending and shear cracks in the column plastic hinge zone.

In comparison to the specimen RC-0, the three strengthened columns specimens showed greater and more stable hysteretic responses in both increasing the energy dissipation capacity as well as minimizing the strength deterioration and stiffness degradation of the column during the reversed cyclic load.

In order to apply the current method in a practical construction field, a manufacturing scheme of the HPFRC by precast in the factory should be investigated in the future since it is not practical to simultaneously mix and apply HPFRC with ready-mixed concrete in the construction field.

Acknowledgements

This research was supported by the Basic Science Research Program through the National Research Foundation of Korea (NRF) funded by the Ministry of Education, Science and Technology (No. 2010-0004419). This study was also supported by research funds from Chosun University, 2011.

References

[1] Paulay T, Priestley MJN. Seismic design of reinforced concrete and masonry buildings. New York: John Wiley and Sons; 1992.
[2] ACI 318-05/318R-05. Building code requirements for structural concrete (ACI 318-05) and commentary (ACI 318R-05). Michigan: American Concrete Institute, Farmington Hills; 2005.
[3] Cho CG, Hotta H, Takiguchi K. Compressive strength of concrete in flexural critical region of reinforced concrete beam-column members. Adv Struct Eng 2011;14(6):981–90.
[4] Priestley MJN, Seible F, Calvi GM. Seismic design and retrofit of bridges. John Wiley and Sons; 1996. 686p.
[5] Ha GJ, Cho CG. Strengthening of reinforced high-strength concrete beam-column joints using advanced reinforcement details. Mag Concr Res 2008;60(7):487–97.
[6] Mirmiran A, Shahawy M. Behavior of concrete columns confined by fiber composites. J Struct Eng 1997;123(5):583–90.
[7] Fahmy MFM, Wu Z. Evaluating and proposing models of circular concrete columns confined with different FRP composites. Compos Part B: Eng 2010;41(3):199–213.
[8] Zinno A, Lignola GP, Prota A, Manfredi G, Cosenza E. Influence of free edge stress concentration on effectiveness of FRP confinement. Compos Part B: Eng 2010;41(7):523–32.
[9] Realfonzo R, Napoli A. Concrete confined by FRP systems: confinement efficiency and design strength models. Compos Part B: Eng 2011;42(4):736–55.
[10] Saadatmanesh H, Ehsani MR, Li MW. Strength and ductility of concrete columns externally reinforced with fiber composite straps. ACI Struct J 1994;91(4):434–47.
[11] Ascione L, Feo L. Modeling of composite/concrete interface of RC beams strengthened with composite laminates. Compos Part B: Eng 2000;31(6–7):535–40.
[12] Ascione L, Berardi VP, Feo L, Mancusi G. A numerical evaluation of the interlaminar stress state in externally FRP plated RC beams. Compos Part B: Eng 2005;36(1):83–90.
[13] Aprile A, Feo L. Concrete cover rip-off of R/C beams strengthened with FRP composites. Compos Part B:Eng 2007;38(5–6):759–71.
[14] Cho CG, Kwon M, Spacone E. Analytical model of concrete-filled fiber-reinforced polymer tubes based on multiaxial constitutive laws. ASCE J Struct Eng 2005;131(9):1426–33.
[15] Cho CG, Kwon M. Nonlinear failure prediction of concrete composite columns by a mixed finite element formulation. Eng Fail Anal 2011;18:1723–34.
[16] Cho CG, Ha GJ, Kim YY. Nonlinear model of reinforced concrete frames retrofitted by in-filled HPFRCC walls. Struct Eng Mech 2008;30(2):211–23.
[17] Kim YY, Fischer G, Li VC. Performance of bridge deck link slabs designed with ductile Engineered Cementitious Composite (ECC). ACI Struct J 2004;101(6):792–801.
[18] Li VC. From micromechanics to structural engineering – the design of cementitious composites for civil engineering applications. JSCE J Struct Mech Earthquake Eng 1993;10(2):37–48.
[19] Li VC. Post-crack scaling relations for fiber reinforced cementitious composites. ASCE J Mater Civil Eng 1992;4(1):41–57.
[20] Fischer G, Li VC. Effect of matrix ductility on deformation behavior of steel-reinforced ECC flexural members under reversed cyclic loading conditions. ACI Struct J 2002;99(6):781–90.
[21] Fischer G, Li VC. Deformation behavior of fiber-reinforced polymer reinforced Engineered Cementitious Composite (ECC) flexural members under reversed cyclic loading conditions. ACI Struct J 2003;100(1):25–35.